High-frequency EPR on high-spin transitions-metal sites

Mathies, G.

Chapter 3

Multi-frequency EPR study of Fe^{3+} and Co^{2+} in the active site of desulforedoxin

The continuous-wave 275.7 GHz EPR spectra of a frozen solution of desulforedoxin provide the zero-field splitting (ZFS) parameters of the high-spin Fe^{3+} active site: $D = 72 \pm 1$ GHz and $\lambda = 0.074 \pm 0.002$. The X-band spectra of a frozen solution of Co(II)-substituted desulforedoxin at multiple temperatures allow an estimate of the ZFS parameters: $D < -300$ GHz and $\lambda = 0.26$. The typical variation in the geometry of the active site of a protein or enzyme, usually referred to as conformational strain, does not only make the detection of EPR spectra challenging, but also their analysis. The remarkable differences between the ZFS parameters of the high-spin Fe^{3+} site of desulforedoxin, the high-spin Fe^{3+} site of rubredoxin and the high-spin Co^{2+} substituted site of desulforedoxin are discussed.

Guinevere Mathies, Rui M. Almeida, Peter Gast, José J. G. Moura and Edgar J. J. Groenen, *in preparation.*

3.1 Introduction

In many proteins and enzymes the active site contains a paramagnetic transition-metal ion and electron-paramagnetic-resonance (EPR) spectroscopy can provide detailed information on its electronic structure. This makes EPR spectroscopy an invaluable tool in the study of the relationship between structure and function of the active sites in biological molecules. [61–63] Whenever the transition-metal ions carry a spin angular momentum $S > 1/2$ the degeneracy of the magnetic sublevels may already (partly) be lifted in the absence of an external magnetic field. For such systems it is advantageous, or even required, to record EPR spectra at a microwave frequency comparable to or larger than this zero-field splitting (ZFS), and one needs an EPR spectrometer operating at a frequency higher than the standard 9.5 GHz (X band). Fortunately, the last decades have shown a strong increase in the possibilities to perform EPR spectroscopy at higher frequencies.

An EPR spectrum is to be analyzed in terms of its spin-Hamiltonian parameters, which then have to be translated into electronic structure using advanced quantum-chemical methods. Considerable progress has been made with such calculations in recent years, in particular based on density-functional theory, but calculation of the ZFS for transition-metal ions remains still in an exploratory stage, [8] particularly for biological sites. Consequently there is a need for more experimental data on such systems that can be used as benchmarks.

A challenge in high-frequency EPR is to achieve the sensitivity needed to study transition-metal sites in biological molecules. Recently we have demonstrated that, using a single-mode cavity, it is possible to record high-quality EPR spectra in continuous-wave (cw) mode at 275.7 GHz (J band) of mM frozen solutions of the protein rubredoxin, whose active site in the oxidized state contains high-spin Fe^{3+}, see Chapter 2. [64] We were able to detect differences on the order of 1 GHz in the ZFS between rubredoxins from different organisms. Here we study the closely related active site of the protein desulforedoxin by multi-frequency EPR, both in its natural high-spin Fe^{3+} ($S = 5/2$) form and substituted with high-spin Co^{2+} ($S = 3/2$).

The rubredoxin class of small proteins found in sulfur-metabolizing bacteria and archaea is known to participate in electron transport. [10] The rubredoxin active site comprises an iron atom bound in an approximately tetrahedral geometry to four cysteine residues, which occur in two ...x-Cys-x-x-Cys-x... segments. Desulforedoxin is a homodimer consisting of two, 36 amino acid chains [65, 66] and has two equivalent $Fe(S\text{-}Cys)_4$ active sites. The site geometry is again approximately tetrahedral, but the four cysteine residues occur in an ...x-Cys-x-x-Cys-x... and an ...x-Cys-Cys-x... segment. [67]

High-spin Fe^{3+} in a four-sulfur coordination has been studied both theoretically [68–70] and experimentally by several spectroscopic methods, both in model complexes, [71–74] and in rubredoxin. [56–58] High-spin Co^{2+} in a four-sulfur coordination has been studied to a lesser extent. [5, 75–78] Cobalt does not occur as

frequently in biological molecules as iron; yet it can be a rewarding spectroscopic probe, for instance as a substitute for diamagnetic Zn^{2+}. [79]

Desulforedoxin has been investigated by Moura *et al.* by X-band EPR and by Mössbauer spectroscopy. [57, 80] Moura *et al.* also recorded an X-band spectrum of Co(II)-substituted desulforedoxin. [81]

We report cw EPR spectra of a frozen solution of Fe(III)-desulforedoxin at J band and X band. The J-band spectra make it possible to determine the ZFS parameters accurately and reveal a small g-anisotropy. No J-band spectrum could be observed of Co(II)-substituted desulforedoxin. The X-band spectra of a frozen solution of Co(II)-desulforedoxin at multiple temperatures allow an estimate of the spin-Hamiltonian parameters. The typical variation in the geometry of the active site of a protein or enzyme, referred to as conformational strain, does not only make the detection of their EPR spectra challenging, but also complicates the analysis. The differences between the ZFS parameters of the high-spin Fe^{3+} site of desulforedoxin, the high-spin Fe^{3+} site of rubredoxin and the high-spin Co^{2+} substituted site of desulforedoxin are discussed.

3.2 Materials and methods

Desulforedoxin from *Desulfovibrio gigas* was expressed in *E. coli* and purified following a procedure similar to the procedure described in reference 47 for rubredoxin. Reconstitution with Co^{2+} was performed as described in reference 81. All proteins were kept in Tris buffer at pH 7.6. Samples for X-band EPR contained 20% glycerol.

The cw J-band EPR spectra were recorded on an in-house developed spectrometer, [9] using a probe head specialized for operation in cw mode as described in Chapter 2. [64] The effective sample volume, limited by the microwave cavity, is approximately 20 nl. The cw W-band (94.1 GHz) spectra were recorded on a Bruker Elexsys E680 spectrometer using a W-band "ENDOR" probe head with a cylindrical TE_{011} cavity in a CF935W flow cryostat (Oxford Instruments). Pulsed W-band (94.9 GHz) spectra were recorded on an in-house developed spectrometer. [82] The cw X-band spectra were also recorded on a Bruker Elexsys E680 spectrometer, using a TE_{102} rectangular cavity equipped with an ESR 900 Cryostat (Oxford Instruments).

3.3 Results and analysis

3.3.1 Desulforedoxin

Figure 3.1 shows cw J-band spectra of a frozen solution of desulforedoxin at 5 and 25 K. The complex spectrum covers a field range of more than 10 T. The 5 K spectrum shows three signals that lose intensity at elevated temperatures at 1.7 T

and around 4.7 and 6.5 T. These last two signals have a width of almost 1 T. In the 25 K spectrum signals appear around 7.0, 8.4 and 9.0 T.

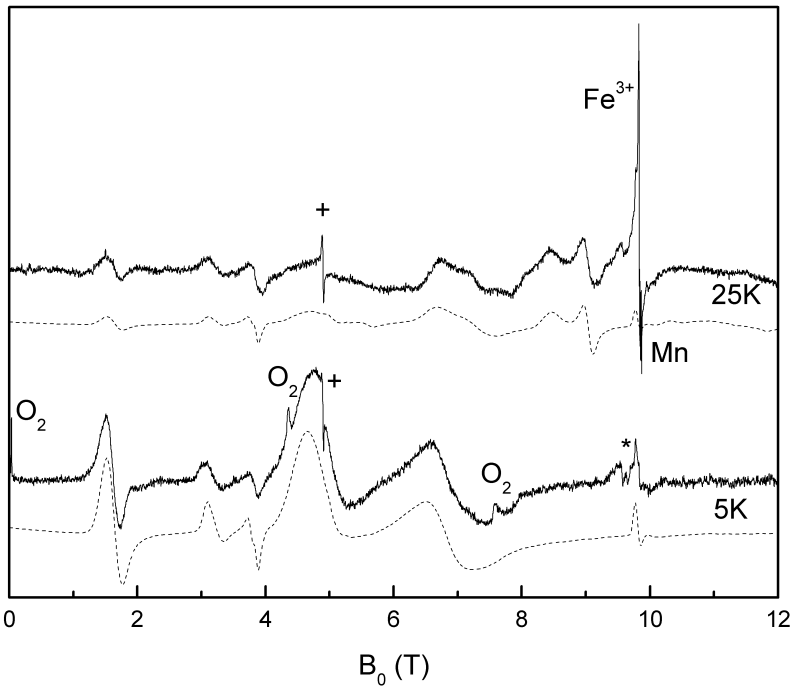

Figure 3.1: J-band cw EPR spectra of a 10 mM frozen solution of desulforedoxin from *D. gigas* at 5 and 25 K. Experimental conditions: modulation amplitude: 3 mT, microwave power: 1 μW, microwave frequency: 275.7 GHz. Solid lines: experimental spectra, dashed lines: spectra calculated using EasySpin and the spin-Hamiltonian parameters given in the text. Experimental spectra are smoothed by adjacent averaging and are baseline corrected at the low- and high-field end. An unknown impurity in the cavity gives a negative peak at 9.6 T, marked with $\star$. The following background signals arise from the frozen solution. At both temperatures a narrow transition at 4.9 T, marked with a +, is due to an unknown impurity. In the 5 K spectrum signals due to oxygen are observed. [51] At 25 K the strong transition around $g = 2$ (9.84 T), which has a shoulder on the low-field side, is due to an unknown rhombic high-spin Fe^{3+} contaminant and a detailed scan of the $g = 2$ region revealed six lines of Mn^{2+}.

Figure 3.2 shows cw X-band spectra of a frozen solution of desulforedoxin at 5, 10 and 80 K. In the spectra three signals, at 86.6, 162 and 369 mT, lose intensity as temperature increases. The signals at 162 and 369 mT are considerably broader than the signal at 86.6 mT. A signal at 116.4 mT remains relatively strong at elevated temperatures.

The following spin Hamiltonian is used to interpret the EPR spectra arising from

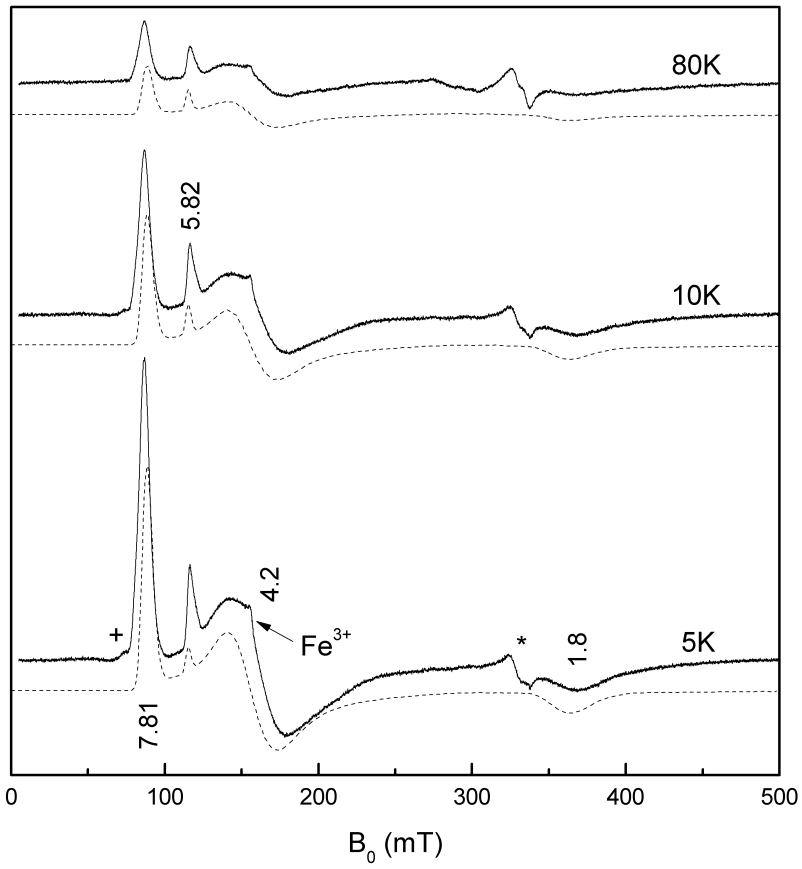

Figure 3.2: X-band cw EPR spectra of a 0.6 mM frozen solution of desulforedoxin from *D. gigas* at 5, 10 and 80 K. Experimental conditions: modulation amplitude: 1 mT, microwave power: 5 and 10 K spectra: 1.3 mW, 80 K spectrum: 20 mW, microwave frequency: 9.491 GHz. Solid lines: experimental spectra, dashed lines: spectra calculated using EasySpin and the spin Hamiltonian parameters determined from the J-band spectra. The signal marked with a $\star$ just below $g = 2$ (331 mT) is due to an impurity in the cavity. The signal marked with a + is an unknown impurity in the frozen solution, which was also observed by Moura *et al.*, [57, 80] and the signal around $g = 4.3$ (157 mT) is due to an unknown rhombic high-spin Fe^{3+} contaminant.

high-spin Fe^{3+}, $S = 5/2$. [3]

$$H = \mu_B \vec{B}_0 \cdot \vec{\vec{g}} \cdot \vec{S} + \vec{S} \cdot \vec{\vec{D}} \cdot \vec{S} \tag{3.1}$$

The first term describes the electron Zeeman interaction. A first-order contribution from spin-orbit coupling induces g-anisotropy, but this anisotropy is expected to be small, since high-spin Fe^{3+} has an S ground state. The second term describes the ZFS, which splits the six magnetic sublevels into three Kramers doublets. The

ZFS-tensor, $\vec{\vec{D}}$, is symmetric, can be taken traceless, and is characterized by two parameters, D and E.

$$D = 3/2D_z,\ E = 1/2(D_x - D_y) \tag{3.2}$$

The rhombicity of $\vec{\vec{D}}$ is given by the ratio $\lambda = E/D$. The principal axes are chosen such that $|D_z| > |D_y| > |D_x|$ and $0 < \lambda < 1/3$.

From X-band EPR and Mössbauer spectra of desulforedoxin, Moura *et al.* estimated λ to be 0.08 and D to be 2 cm^{-1} or 60 GHz, [57, 80, 83] which explains the complexity of the desulforedoxin spectra in Figure 3.1. At J band the two terms in the spin Hamiltonian are comparable in size and the three Kramers doublets are intertwined. Analysis of the J-band spectra was performed by comparison to spectra calculated by numerical diagonalization of the spin Hamiltonian using the EPR simulation package EasySpin, [6] taking the parameters of Moura *et al.* as a starting point. The principal axes of the g-tensor are assumed to be collinear with those of the D-tensor. The experimental J-band spectra were best reproduced taking $D = 72$ GHz and $\lambda = 0.074$. Increasing the principal values of the g-tensor to above the free electron value improved the simulation: $g_x, g_y = 2.020$, $g_z = 2.025$. To reproduce the width and shape of the resonances in the J-band spectra a strain in D and E of 20% was taken into account using a first-order approximation,[1] cf. Discussion.

At X band the ZFS is larger than the microwave quantum of 9.5 GHz and only intra-doublet transitions can be observed. The system approaches the regime where each of the three Kramers doublets can be approximated as an effective $S' = 1/2$ system. [7] In this regime the anisotropic Zeeman splitting of each doublet is reflected in effective g'-values, g'_x, g'_y and g'_z, which depend on the g-values and λ, but not on D. The signals at the effective g'-values of 7.8, 4.2 and 1.8, which lose intensity at elevated temperatures, arise from the lowest doublet, $\pm 1/2$. The signal at $g' = 5.8$ is found to arise from the middle $\pm 3/2$-doublet. The dashed lines in Figure 3.2 are spectra calculated using the parameters determined from the J-band spectra. In these spectra the line broadening was simulated by using a Gaussian distribution in λ of FWHM = 0.035, which corresponds to a distribution width of approximately 20% in D and E. The experimental spectra are reproduced, but there are small differences, on the order of 1 mT, between the calculated and experimental fields of resonance.

3.3.2 Co(II)-desulforedoxin

Figure 3.3 shows cw X-band spectra of a frozen solution of Co(II)-desulforedoxin at 5, 10, 25 and 40 K. At 5 K three transitions can be observed, around 110, 290,

[1] See the online documentation on EasySpin.

and 420 mT. The middle- and high-field transitions are very broad and overlap. Upon increase of the temperature these three transitions lose intensity. At 25 and 40 K a new transition can be observed around 192 mT. The minimum found at low temperature around 420 mT shifts to around 380 mT at elevated temperatures. The transition around 110 mT preserves some of its intensity at 40 K and broadens.

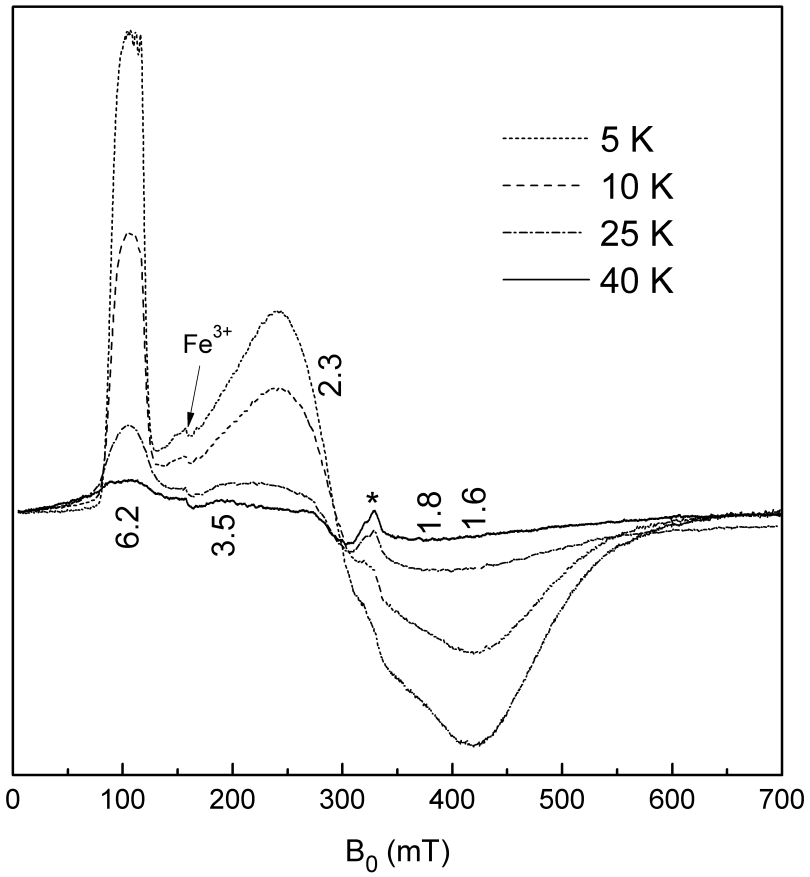

Figure 3.3: X-band cw EPR spectra of a 0.7 mM frozen solution of Co(II)-desulforedoxin from *D. gigas* at 5, 10, 25 and 40 K. Experimental conditions: modulation amplitude: 1.5 mT, microwave power: 200 mW, microwave frequency: 9.495 GHz. A baseline was subtracted. The signal marked with a $\star$ around $g = 2$ (331 mT) is due to an impurity in the cavity. The signal around $g = 4.3$ (157 mT) is due to an unknown rhombic high-spin Fe^{3+} contaminant.

At J band no spectrum of Co(II)-desulforedoxin could be detected. At W band an electron-spin-echo (ESE) detected EPR spectrum was observed at 1.7 K, shown in Figure 3.4. A spin echo due to Co(II)-desulforedoxin was detected at magnetic fields above 1.1 T. The echo amplitude reached a maximum around 3.2 T. An attempt was made to measure the cw spectrum of a 4 mM frozen solution of Co(II)-desulforedoxin

at W band. At 6.5 K a peak around 1 T showed up very weakly.

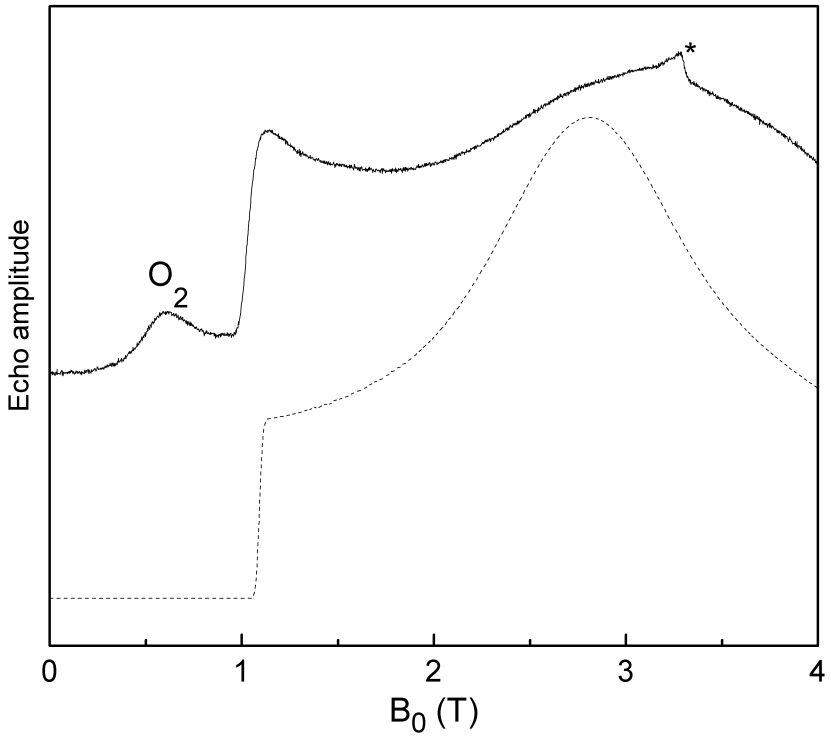

Figure 3.4: W-band ESE-detected EPR spectra of a 0.7 mM frozen solution of Co(II)-desulforedoxin from *D. gigas* at 1.7 K. Experimental conditions: a two-pulse Hahn echo is generated by the pulse sequence $\pi/2 - \tau - \pi = 70 - 405 - 140$ ns, repetition time: 1 ms, microwave power: 1 mW, microwave frequency: 94.9 GHz. Solid line: experimental spectrum, dashed line: spectrum calculated using EasySpin and the spin-Hamiltonian parameters given in the text. The signal around 0.6 T results from oxygen in the frozen solution. [51] The signal marked with a $\star$ at $g = 2$ (3.39 T) results from an unknown impurity.

To interpret the high-spin Co^{2+}, $S = 3/2$, spectra a term describing the hyperfine interaction with the ^{59}Co nucleus ($I = 7/2$) should be added to the spin Hamiltonian 3.1.

$$H = \mu_B \vec{B_0} \cdot \vec{\vec{g}} \cdot \vec{S} + \vec{S} \cdot \vec{\vec{D}} \cdot \vec{S} + \vec{S} \cdot \vec{\vec{A}} \cdot \vec{I} \tag{3.3}$$

The ground state of high-spin Co^{2+} is an F state. A first-order contribution from spin-orbit coupling induces considerable g-anisotropy. The ZFS, which is large, typically hundreds of GHz, splits the four energy levels of the ground state into two Kramers doublets. The contribution of a nuclear Zeeman interaction by cobalt can be neglected.

Analysis of the X-band spectra is performed under the assumption that the effective $S' = 1/2$ description of the doublets is valid. For an $S = 3/2$ system the effective g'_i-values are related to the g_i-values by [7, 84, 85]

$$\begin{aligned} g'_x &= g_x \left(1 \pm \frac{1-3\lambda}{\sqrt{1+3\lambda^2}}\right) \\ g'_y &= g_y \left(\pm 1 + \frac{1+3\lambda}{\sqrt{1+3\lambda^2}}\right) \\ g'_z &= g_z \left(\mp 1 + \frac{2}{\sqrt{1+3\lambda^2}}\right) \end{aligned} \tag{3.4}$$

The upper signs refer to the $\pm 1/2$ doublet and the lower signs to the $\pm 3/2$ doublet. Note that these relations presume that the principal axes of the g- and D-tensor are collinear.

The transitions observed in the 5 K spectrum, at effective g'-values 6.2, 2.3 and 1.6 respectively, are due to the anisotropic splitting of the lower Kramers doublet. At 25 and 40 K the spectra are dominated by three transitions at effective g'-values 6.2 (110 mT), 3.5 (192 mT) and 1.8 (380 mT), which arise from the upper Kramers doublet. Following Equation 3.4, the transition at $g' = 3.5$ must be the g'_x transition of the $\pm 1/2$ doublet. Hence, the $\pm 1/2$ doublet is higher in energy and D is negative. Equation 3.4 and a minimization procedure were used to estimate the values of λ and g_x, g_y, and g_z from the six observed effective g'-values. This gave $\lambda = 0.26$, $g_x = 2.9$, $g_y = 2.4$, and $g_z = 2.2$. These values are, together with a large, negative D, used to simulate the Co(II)-desulforedoxin spectra with EasySpin, [6] as shown for the 5 K spectrum in Figure 3.5. The shape of the experimental spectra is qualitatively reproduced by the simulation, but fine tuning is clearly needed. This has not been pursued, see Discussion.

To simulate line broadening in the X-band spectra, a Gaussian distribution in λ of FWHM 0.035 was used. The broadening of the $g'_z(\pm 3/2)$ transition is mainly due to a (partially resolved) hyperfine interaction with the ^{59}Co nucleus of approximately $A_z = 150$ MHz.

The dashed spectrum in Figure 3.4 is the absorption spectrum calculated using EasySpin and the spin-Hamiltonian parameters estimated from the frozen solution cw X-band spectra. It reproduces qualitatively the ESE detected EPR spectrum, i.e., the onset of the spin echo at 1.1 T, which corresponds to $g'_z(\pm 3/2) = 6.2$, and the broad field range over which an echo is observed.

3.4 Discussion

The cw J-band spectra of the frozen solution of desulforedoxin are well reproduced by spectra calculated from numerical diagonalization of the spin Hamiltonian, [6]

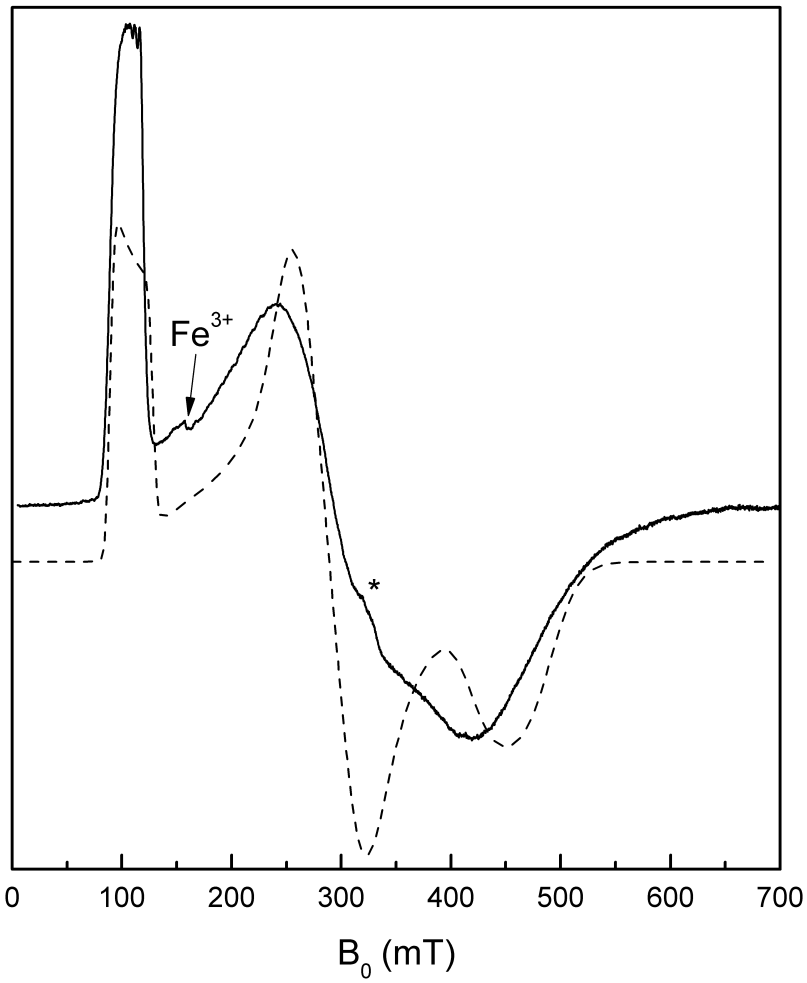

Figure 3.5: X-band cw EPR spectrum of a 0.7 mM frozen solution of Co(II)-desulforedoxin from *D. gigas* at 5 K. Solid line: experimental spectrum, dashed line: spectrum calculated using EasySpin and the spin-Hamiltonian parameters given in the text. The signal marked with a $\star$ around $g = 2$ (331 mT) is due to an impurity in the cavity. The signal around $g = 4.3$ (157 mT) is due to an unknown rhombic high-spin Fe^{3+} contaminant.

see Figure 3.1, optimally with the ZFS parameters $D = 72 \pm 1$ GHz and $\lambda = 0.074 \pm 0.002$, and a small g-anisotropy, $g_x, g_y = 2.020 \pm 0.001$, $g_z = 2.025 \pm 0.005$. The uncertainty in a parameter was estimated from the calculated shift of the J-band resonances upon a change in that parameter. Because the microwave quantum ($\nu = 275.7$ GHz) is larger than the ZFS, inter-doublet transitions are possible and the spectrum is very sensitive to both E and D. An X-band spectrum, on the other hand, depends on $\lambda = E/D$, and D needs to be estimated via an elaborate

temperature study. [56] Moreover, at X band the small g-anisotropy of high-spin Fe^{3+} is not resolved.

Conformational strain is typical for proteins and enzymes. The geometrical variations affect the electronic structure of active sites, which translates into a distribution in the ZFS parameters for high-spin Fe^{3+} [58, 86] and in a distribution in the ZFS parameters and the principal values of the g-tensor for high-spin Co^{2+}. This does not only result in line broadening, which can make it difficult to detect the EPR spectrum of a biological site, but it may also deform the spectrum, which complicates its analysis. Particularly, if a change in a spin-Hamiltonian parameter results in a large change of the transition probability, strain can result in a shift of what appears to be the average field of resonance in the experimental EPR spectra.

In order to reproduce the line widths in the experimental J-band spectra of desulforedoxin, the spectra were simulated using EasySpin with a strain of about 20% in D and E. A first-order approximation is used, in which the spectrum was convoluted with a Gaussian of a width proportional to the derivative of the resonance field of a given transition with respect to, for instance, D; the proportionality constant is chosen by the user. This approximation is valid if the strain is much smaller than the parameter itself. In the high-field limit, $\mu_B \vec{B}_0 \cdot \vec{\vec{g}} \cdot \vec{S} \gg \vec{S} \cdot \vec{\vec{D}} \cdot \vec{S}$, where the magnetic field at which the resonances in a frozen solution spectrum are observed depends linearly on the principal values of the D-tensor, [45] the approximation may also be valid for larger strains in D and E, if the transition probability does not depend strongly on these parameters. This was found to be the case for Fe(III)-rubredoxin, $D = 48$ GHz, by comparison to spectra calculated using a distribution in D and E. [64] For desulforedoxin, $D = 72$ GHz, such a comparison was not feasible, because the calculation of the individual spectra is too time consuming.

The X-band spectra of Fe(III)- and Co(II)-desulforedoxin are typical of a site that experiences large conformational strain: the resonances at low g-values are very broad, while the resonances at high g-values are narrower. The distributions in g'_x, g'_y and g'_z are of similar width, but the distribution in the resonance fields will be broader for the smaller g'_i-values. To simulate the experimental X-band spectra of both sites, the effect of conformational strain was taken into account by using a Gaussian distribution in λ. For Fe(III)-desulforedoxin the experimental line width was well reproduced, but small deviations in the resonance fields remained between the experimental spectra and the calculated spectra when using the spin-Hamiltonian parameters determined from the J-band spectra. For Co(II)-desulforedoxin the line width is poorly reproduced and it is hard to say if the resonance fields are reproduced properly. Of course, a proper simulation of the Co(II)-desulforedoxin X-band spectra requires not only a distribution in λ, but also in g_x, g_y and g_z.

For Co(II)-desulforedoxin not only the effect of conformational strain, but also the spin-Hamiltonian parameters are uncertain. The values of the parameters used in the simulation of the X-band spectra were merely an estimate. Following Equa-

tion 3.4 the only possible assignment for the peak observed at $g' = 3.5$ at elevated temperatures is the g'_x transition of the $\pm 1/2$ doublet, making $D < 0$. However, the value of 2.9 for g_x, which has to be invoked to fit the observed $g'_x(\pm 1/2) = 3.5$ and, particularly, the $g'_x(\pm 3/2) = 2.3$ transition, is unusually large. [87, 88] Besides the very large ZFS and the difficulties encountered when simulating the effects of conformational strain, there is a third reason that the X-band spectrum of Co(II)-desulforedoxin can not provide more accurate information on the electronic structure. The covalent character of the bonding with the soft sulfur ligands may cause the principal axes of the D- and g-tensors to be non-collinear, [8, 89, 90] which implies that the g-values can not be calculated from Equation 3.4. Moreover, analysis by comparison to spectra calculated by numerical diagonalization of the spin Hamiltonian is not an option, since the relative orientation of the principal axes of interaction tensors is now a variable.

High-frequency EPR spectra of Co(II)-desulforedoxin could be helpful. First, they can provide information on the relative orientation of the principal axes of the D- and g-tensors. At X band the direction of the effective magnetic field is dominated by the D-tensor. If spectra are recorded at higher frequency and higher magnetic field, the influence of the Zeeman interaction on the direction of the effective magnetic field becomes noticeable. Also, at higher frequency deviations from the effective $S' = 1/2$ picture start to occur, an effect that was used in the multi-frequency EPR study of a high-spin Co^{2+} complex to estimate D. [5] Or, ideally, the regime $\nu \approx D$ is reached and inter-doublet transitions become possible. [91–94]

Unfortunately no spectrum of Co(II)-desulforedoxin could be observed in cw at J-band. The ESE-detected W-band spectrum corroborates our interpretation of the cw X-band spectra, but fine tuning of the parameters based on this spectrum is complicated by anisotropic relaxation times. No high-frequency studies of high-spin Co^{2+} in the active site of a protein are found in literature. The reason that high-frequency spectra of Co(II)-substituted desulforedoxin, and of biological high-spin Co^{2+} systems in general, are hard to come by is the large g-anisotropy. Conformational strain results in a distribution in g_i, on top of a distribution in D and E, which, as long as the regime $\nu \approx D$ is not reached, causes a severe broadening of the resonances, particularly at high magnetic fields. Hence, the absence of a spectrum at J band suggests that $|D|$ is larger than about 300 GHz.

If we compare the spin-Hamiltonian parameters of the active site of desulforedoxin to those of the active site of rubredoxin, we notice remarkable differences. First, the rhombicity of the ZFS-tensor of the high-spin Fe^{3+} sites differs considerably for desulforedoxin and rubredoxin. The D and λ of rubredoxin from *D. gigas* are known to be 48.5 GHz and 0.26, see Chapter 2, [64] while we find $D = 72$ GHz and $\lambda = 0.074$ for desulforedoxin. Second, while D is positive for the Fe^{3+} sites, D is negative for the Co(II)-substituted active site of desulforedoxin and, moreover, the rhombicity of Co(II)-desulforedoxin is comparable to that of the Fe^{3+} site of rubre-

doxin: $D < -300$ GHz and $\lambda = 0.26$. At this point it would be desirable to know the ZFS parameters of Co(II)-substituted rubredoxin, but, unfortunately, we were not successful in obtaining an EPR spectrum of Co(II)-rubredoxin, despite considerable effort, cf. Appendix C. However, the absence of an EPR spectrum suggests a $\lambda \approx 0$ and $D < 0$. In this situation a transition within the lowest doublet is (almost) forbidden and at elevated temperatures, where the higher doublet becomes populated, the transitions within this doublet may broaden strongly due to fast relaxation.

The electronic structure of sulfur-coordinated transition-metal sites is known to depend on the structure of the site beyond the first coordination sphere. [68–70, 74, 95] For both rubredoxin and desulforedoxin from *D. gigas* the structures are known to a high resolution. [14, 46, 66] The structure of Co(II)-substituted rubredoxin is indistinguishable from the structure of Fe(III)-rubredoxin by X-ray diffraction. [96] No X-ray diffraction study of the structure of Co(II)-substituted desulforedoxin has been performed, but we will assume that its structure is the same as that of Fe(III)-desulforedoxin.

Figure 3.6a shows the structure of the active site of rubredoxin. The $Fe(SC)_4$ geometry is approximately what is referred to in reference 70 as the $D_{2d}(1)$ or double-bird geometry. This conformation is the combined result of the site being built up from four cysteine residues on two amino acid strands and the sulfur-lone-pair repulsion. The FeS_4 core is elongated from T_d symmetry (two smaller angles and four larger ones). [95] Figure 3.6b shows the structure of the active site of desulforedoxin. The angle S-Fe-S involving Cys28 and Cys29 is relatively large, 121.5°, due to the adjacency of the two cysteines, and C_9-S_9-Fe-S_{29}-C_{29} is not able to assume the bird geometry on the Cys29 side.

Interpretation of the ZFS parameters in relation to the structure of the active sites is far from straightforward. Ligand-field considerations concerning the metal *d*-orbitals are of limited applicability because of the significant (anisotropic) covalency of the metal-sulfur bonds. Recently, the experimental ZFS parameters of a number of high-spin Co^{2+} complexes have been well reproduced by correlated ab-initio calculations. [97] In particular, for the truncated double-bird core of the complex $[Co(SPh)_4]^{2-}$ a large negative D and $\lambda = 0$ were calculated. [76] The approximate double-bird geometry of the rubredoxin active site suggests similar ZFS parameters for the high-spin Co^{2+} site, which would be in line with the ZFS parameters predicted from the absence of an EPR spectrum. In this respect the $\lambda = 0.26$ of the Co(II)-substituted active site of desulforedoxin, which is considerably more asymmetric than the rubredoxin site, is in line with expectations.

The $\lambda = 0$ for the double-bird geometry or D_{2d} symmetry of the Co^{2+} site of the $[Co(SPh)_4]^{2-}$ complex does not merely follow from the ab initio calculations. All interaction tensors must be axial if the symmetry of the site is S_4 or higher. From this perspective the $\lambda = 0.26$ observed for high-spin Fe^{3+} rubredoxin is remarkable. Moreover, a ZFS tensor that is closer to axial, $\lambda = 0.074$, is observed for high-spin Fe^{3+} desulforedoxin. These observations illustrate how difficult it is to predict the

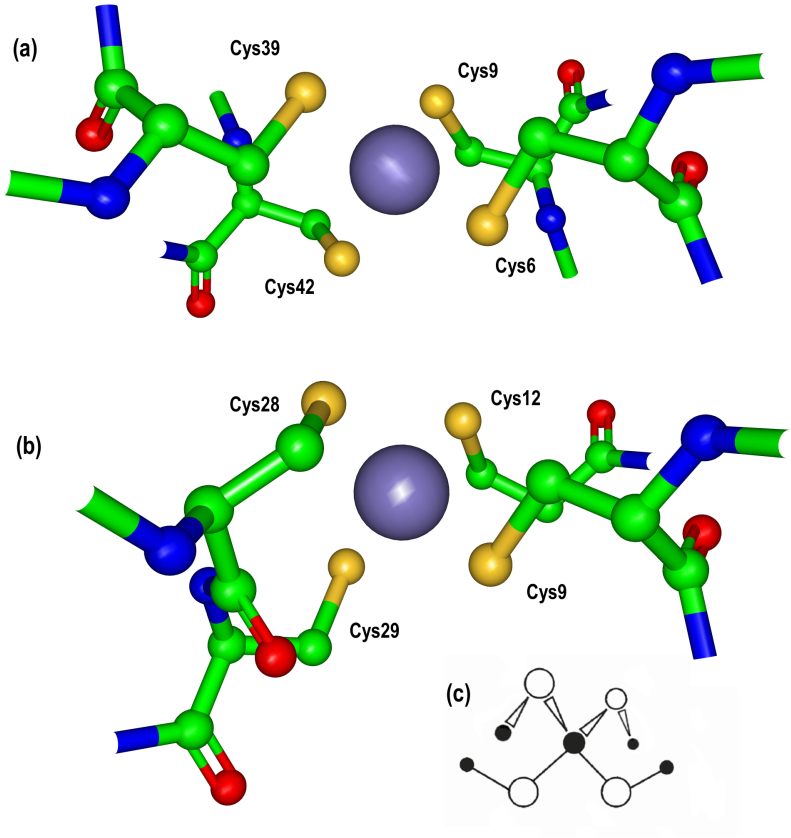

Figure 3.6: a) The structure of the active site of rubredoxin from *D. gigas*. b) The structure of the active site of desulforedoxin from *D. gigas*. c) Schematic drawing of the double-bird geometry.

effects of deviations from a presumed symmetry of a site on its electronic structure.

The deviations of symmetry in the sites of rubredoxin and desulforedoxin affect the electronic structure differently, depending on whether the site is occupied by high-spin Co^{2+} ($3d^7$ configuration) or high-spin Fe^{3+} ($3d^5$ configuration). These differences arise because the former has a ^{4}F ground state, while the latter has a ^{6}S ground state. The in-state orbital angular momentum of the high-spin Co^{2+} may be quenched by the low symmetry of the site, but is easily restored by mixing of the ground state with nearby excited states and a g-anisotropy and large ZFS are expected. [84] On the other hand, for high-spin Fe^{3+} no in-state orbital angular momentum and no ligand field excited states of the same multiplicity are present. The origin of the observed ZFS, which is much smaller than for high-spin Co^{2+}, lies mainly in anisotropy in the covalency, which even reverses the sign of D. [71, 72, 98]

3.5 Conclusion

High-frequency EPR spectroscopy provides valuable information on the electronic structure of high-spin transition-metal sites in biological systems. At the same time, the observation and analysis of the spectra is not straightforward, particularly in the case of high-spin Co^{2+}. Attempts to interpret the ZFS tensors and g-anisotropy observed for high-spin Fe^{3+} and high-spin Co^{2+} in the active sites of desulforedoxin and rubredoxin illustrate the necessity of further development of advanced quantum-chemical calculations, which can interrelate the geometric structure and electronic structure of these active sites.

3. Multi-frequency EPR study of Fe^{3+} and Co^{2+} in the active site of desulforedoxin